

Highly Impact-Resistant Silk Fiber Thermoplastic Composites

Van Vuure, Aart Willem; Mosleh, Yasmine; Vanderbeke, Jan; Verpoest, Ignaas

DOI

[10.1002/adem.202300080](https://doi.org/10.1002/adem.202300080)

Publication date

2023

Document Version

Final published version

Published in

Advanced Engineering Materials

Citation (APA)

Van Vuure, A. W., Mosleh, Y., Vanderbeke, J., & Verpoest, I. (2023). Highly Impact-Resistant Silk Fiber Thermoplastic Composites. *Advanced Engineering Materials*, 25(20), Article 2300080. <https://doi.org/10.1002/adem.202300080>

Important note

To cite this publication, please use the final published version (if applicable). Please check the document version above.

Copyright

Other than for strictly personal use, it is not permitted to download, forward or distribute the text or part of it, without the consent of the author(s) and/or copyright holder(s), unless the work is under an open content license such as Creative Commons.

Takedown policy

Please contact us and provide details if you believe this document breaches copyrights. We will remove access to the work immediately and investigate your claim.

Highly Impact-Resistant Silk Fiber Thermoplastic Composites

Aart Willem Van Vuure, Yasmine Mosleh,* Jan Vanderbeke, and Ignaas Verpoest

Silk fibers combine good stiffness and strength with a very high strain to failure and are as such highly promising to realize composites with high impact resistance. It is shown that to realize this potential it is quite beneficial to employ matrix materials of high strain to failure, particularly thermoplastic matrices. High impact resistance is thus achieved, well above the values for the pure matrices. Below the glass-transition temperature of the thermoplastic matrix, the impact energy absorption decreases. The adhesion between fiber and matrix also plays a significant role; lower adhesion typically increases the low-velocity penetration impact resistance, due to the spread of damage. Finally, the fiber architecture is pivotal; when a woven fabric is used which is unbalanced in strength, the impact resistance reduces in correspondence with the weakest material direction. A quasi-isotropic layup has a lower capacity for deformation than a balanced woven configuration which likely explains the observed lower penetration impact resistance.

silk fiber composites with high strain to failure are obtained with promising prospects for impact resistance. This aspect has been much less published about, where most papers work with relatively low strain to failure matrices^[3–6] and is further explored in this article.

This article focuses on low-velocity impact (impact velocity lower than 10 m s^{-1}) of composite plates and considers the necessary energy needed for full penetration. Of course other important impact properties are damage tolerance, i.e., amount of damage caused by impact and residual mechanical properties, or alternatively amount of damage at a prescribed impact energy or impact energy needed for first (visible) damage, etc. These impact characteristics may have conflicting requirements with respect to the necessary

material properties, e.g., low fiber–matrix adhesion may result in high-penetration-impact resistance, but at the same time in low residual mechanical properties of the composite.

In this article, the influence of ingredient material properties on the composite penetration impact resistance is investigated. The important ingredient material properties are fiber toughness, matrix toughness, and fiber–matrix interfacial adhesion, as well as fiber volume fraction, fiber stiffness, fiber length, and fiber architecture. The important energy absorption mechanisms during low-velocity penetration impact are fiber failure, matrix failure, fiber–matrix debonding, fiber pullout, and delamination. During plate impact, also the plate bending stiffness is important (e.g., a function of plate thickness), determining, e.g., the amount of elastic energy stored and released during the impact event and the amount of deflection. During high speed impact, other phenomena like shock waves and localization of damage among others due to the short event time play an important role.


A literature survey was done to highlight the importance of material properties for low-velocity-impact penetration resistance. In the following, findings are summarized. The effect of fiber toughness is not so well documented, probably because the traditional reinforcement fibers are all relatively brittle fibers (with a typical strain to failure between 1% and 3%), in contrast to the silk fibers in this article (strain to failure about 20%). In a previous publication^[7] on annealed steel fiber composites, it was shown that tough fibers, with a high energy absorption in a tensile test (particularly by high strain to failure), will result in higher penetration impact resistance, particularly through plastic deformation of the fiber. The used steel fibers had strain to failure close to 20% as well.

1. Introduction

Silk fibers from the *Bombyx mori* caterpillar are known for a unique combination of good stiffness (modulus 16 GPa) and strength (600–750 MPa) and a high strain to failure (around 20%).^[1] This means that the fibers have an intrinsic high toughness (certainly in tension) and could be interesting reinforcement materials in polymer composites. According to a literature survey in a parallel publication by the same authors,^[2] there has been interest in the use of silk as a reinforcement fiber in composites. The parallel study concludes that, especially when incorporated in thermoplastic matrices of high strain to failure,

A. W. Van Vuure, J. Vanderbeke, I. Verpoest
Department of Materials Engineering
Katholieke Universiteit Leuven
Kasteelpark Arenberg 44, bus 2450, B-3001 Leuven, Belgium

Y. Mosleh
Department of Engineering Structures
Faculty of Civil Engineering and Geosciences
TU Delft
2628 CN Delft, The Netherlands
E-mail: y.mosleh@tudelft.nl

 The ORCID identification number(s) for the author(s) of this article can be found under <https://doi.org/10.1002/adem.202300080>.

© 2023 The Authors. Advanced Engineering Materials published by Wiley-VCH GmbH. This is an open access article under the terms of the Creative Commons Attribution License, which permits use, distribution and reproduction in any medium, provided the original work is properly cited.

DOI: 10.1002/adem.202300080

It is generally believed that matrix toughness will play a positive role in penetration impact resistance,^[8–12] due to the possibility of energy dissipation by plastic deformation of the matrix; this is why it is generally understood that thermoplastic composites will be tougher than thermoset composites. This effect is not clear-cut though, as, e.g., brittle matrices may allow for more energy absorption by delamination.^[13,14] Other publications^[15,16] emphasize that matrix toughness is particularly beneficial for damage tolerance, i.e., residual mechanical properties after impact.

The effect of fiber–matrix adhesion on penetration impact resistance is not particularly well documented, although it is known in the composites community that panels for ballistic penetration impact resistance are typically made with a low adhesion strength; this allows for energy absorption by fiber debonding and subsequent fiber pullout as well as for large-scale delaminations; delaminations are a combination of fiber–matrix debonding and matrix failure. Fiber debonding also allows for reduction of stress concentrations around the fibers, delaying fiber breakage. By a low adhesion, damage can spread over a large volume and energy absorption is high. It can be argued that this is the case for any combination of fiber and matrix toughness. In ref. [17], it is, e.g., found that tough metal fibers in a brittle glass matrix give a higher composite toughness when the adhesion is low. A similar observation about the level of adhesion will be made in this article. It can be argued that there will be some optimum minimum adhesion strength for penetration impact resistance. At too low adhesion, too little energy would be absorbed by fiber debonding and fiber pullout.

With respect to the effect of fiber volume fraction, it can be said that in principle higher fiber volume fraction will lead to higher penetration impact resistance for brittle matrices; for tough matrices, e.g., thermoplastic matrices, this is not so clear-cut.

The effect of fiber stiffness is typically a stiffening effect of the composite, which typically leads to lower deflections during plate impact and localization of damage with associated lower penetration impact resistance,^[18] although in theory fiber toughness might increase. The plate stiffening effect is similar as in case of higher plate thickness.^[18,19]

The effect of fiber length is rather straightforward; it is generally accepted that longer fibers lead to higher composite toughness and penetration impact resistance (e.g., ref. [20]), with best performance for continuous fiber composites.

Finally, the fiber architecture plays an important role. Next to influencing composite stiffness as described above, fiber orientation and distribution is very important. Cracks propagate depending on relative values of fiber, matrix, and interface fracture toughness, and fibers can operate as crack stoppers. It is, e.g., often observed that when comparing woven configurations to unidirectional (UD)-laminated composites, UD-laminated composites have a lower interlaminar fracture toughness and can thus by delamination spread the impact energy over a larger volume of the composite with associated increase in penetration impact resistance.^[15,21]

This article focuses on the effects of matrix toughness (strain to failure), interfacial adhesion strength and fiber architecture on the low-velocity penetration impact resistance of silk fiber composites. Initial results^[22] already demonstrated the potential of tough silk fibers to provide impact-resistant composites, as

compared to the state of the art. Impact-penetration-resistance values between two to three times as high as for self-reinforced polypropylene composites, known as very tough and impact-resistant materials,^[23] were obtained.

2. Experimental Section

2.1. Materials

Two twill silk weaves were provided by Sport Soie (France). The properties of the silk fabrics are listed in **Table 1** (evaluated at KU Leuven).

The silk twill weave (2/2) was balanced with equal number of fibers in the weft and in the warp direction. The silk weave (5/3) was unbalanced as 60 wt% of silk was in the warp yarns and only 40% in the weft yarns. On top of the unbalance, the weft yarns were heavily twisted up to 2850 twists per meter. The silk weaves were degummed at the company before delivery.

Polybutylene succinate (PBS), tradename Bionolle 1001, and polybutyl succinate/adipate (PBSa), tradename Bionolle 3001, were provided by Showa High Polymer (Japan) and delivered as blown film of 30 μm thickness.

Copolypropylene (Co-PP) was supplied by Amcor Flexibles, Belgium, as 60 μm film. Pre-stretched polypropylene (PP) film of 50 μm thickness was provided by Curv, Germany. Two grades of Bynel polyolefins were provided by DuPont, Belgium, and extruded by Amcor Flexibles into thin film of 60 μm . The grades used were Bynel 50E725, a maleic anhydride–modified polypropylene (PP-g-MA), and Bynel 40E529, a maleic anhydride–modified high-density polyethylene (HDPE-MA). Polycaprolactone film (grade CAPA FB450–60 μm) was provided by Solvay, Belgium. Ecoflex F BX 7011, a biodegradable polytetramethylene adipate terephthalate (PTMAT), from BASF was supplied by Oerlemans Plastics, The Netherlands. Earthfirst polylactic acid (PLA) film (100 μm) was provided by Sidaplast, Belgium. Physical properties of the thermoplastic polymer matrix materials are given in **Table 2**. Data were taken from the datasheets of the suppliers; some data were confirmed by mechanical testing at KU Leuven. The epoxy resin was supplied by MC Technics of Visé, Belgium. It concerned a Novolac epoxy, which contained two epoxide groups per epoxy molecule and was formulated with 5 parts resin LMB 6305 and 1.5 parts ARADUR(HY) 5021 BB hardener.

Table 1. Silk fabric properties for the silk twill (2/2) and silk twill (5/3) weave.

		Twill (2/2) weave	Twill (5/3) weave
Areal density	g m^{-2}	78	70
Tex warp	g km^{-1}	7	3.9
Warp density	picks cm^{-1}	56	100
Twist warp	twists m^{-1}	100	100
Tex weft	g km^{-1}	10.9	4.1
Weft density	ends cm^{-1}	35	66
Twist weft	twists m^{-1}	100	2850

Table 2. Polymer matrix properties; physical and mechanical properties.

Material	Density [g cm ⁻³]	MFI (230 °C, 2.16 kg) [g 10 min ⁻¹]	Young's modulus [MPa]	Strength at break [MPa]	Elongation to failure [%]
Epoxy	1.3	/	2000	60–70	4
PBS	1.26	1.5	510	57	700
PBSa	1.23	1.5	330	43	900
PCL	1.15	<4	elastomer-like	/	650
PTMAT	1.26	4	elastomer-like	38	700
PLA	1.25	6	3450	60	6
Co-PP	0.89	4.5	400	26	480
PP	0.91	/	2000	42	475
PP-g-MA	0.89	3	400	18	475
HDPE-MA	0.94	3.5	300	15	820

2.2. Composite Preparation

Before composite production, the thermoplastic films were dried overnight at 50 °C together with the silk. Composite laminates were made by compression molding in a hot press. The layup was prepared by stacking the dried polymer films and silk textiles in the required ratio to obtain the targeted fiber volume fraction of 50% and a panel thickness of 2 mm. **Table 3** shows the compression molding parameters. Some polymer plates of 2 mm thickness were prepared in similar fashion as well, to allow comparative testing. Compression molding temperature was set higher than the melting temperature of the thermoplastic matrix and was typically kept below 160 °C to avoid degradation of the silk. This could be detected visually as the silk fabric would turn from white to yellow. For the (0,90)_s silk weave composites, a layup was chosen where the warp direction of the weaves was put in the same direction. Quasi-isotropic silk weave composites were produced by a symmetric sequence of silk twill (2/2) weaves where half of the weaves were turned by 45° with respect to the 0/90 weaves. The composite plate was heated with 5 °C min⁻¹ while under pressure, held for a certain amount of time under

Table 3. Processing parameters for silk fiber composites using different polymer matrices. Melting temperature and some glass-transition temperatures from supplier datasheets are included in the table.

Polymer Matrix	T _g [°C]	T _m [°C]	Compression T [°C]	Hold time [min]	Effective pressure [bar]
Epoxy			125	60	6
PBS	-34	113	130	5	15
PBSa		95	120	5	15
PCL		60	120	5	15
PTMAT		115	130	5	15
PLA		175	185	10	15
CoPP		125	150	10	15
PP	-15	165	170	10	15
PP-g-MA	-5	143	155	5	15
HDPE-MA		135	145	5	15

pressure at the maximum temperature, and cooled down to room temperature under pressure at 5 °C min⁻¹ (see Table 3). This is to achieve full wetting of the individual silk fibers.

Epoxy film was made in-house on a prepregging apparatus using the Novolac epoxy resin. The heating unit was set to 80 °C and the cooling table to 10 °C. A film thickness of 0.3 mm was prepared and the material was cut to suitable lengths. To increase shelf life sheets were stored in a freezer at approximately -18 °C. For the epoxy matrix composite samples, vacuum was used during compression molding.

2.3. Low-Velocity-Impact Testing

Impact properties were determined by two falling weight impact setups. In such a test, plate-type test specimens are punctured at their center using a striker, guided by rails, oriented perpendicular to the test specimen surface. The first setup was mounted on a home-made impact machine. For the second setup, a CEAST Fractovis 6789 impact machine with temperature chamber was used. The resulting force–time diagram and striker displacement–time diagram were recorded automatically. The force was measured by a load cell in the striker; the displacement was measured by a laser device tracking the position of the impactor. The laser reference point was rigidly mounted on the impact head, to record the displacement of the impactor itself, for both setups. The test specimen was clamped during the test. The two different setups used are described in **Table 4**; the first used a large clamping frame (diameter circular impact area 80 mm) and a small hemispherical impact point (diameter 16 mm) and the second used a small clamping frame

Table 4. Main parameters of the two low-velocity-impact setups used in this research.

Low velocity impact setups; circular test area; hemispherical striker	Setup 1	Setup 2
	Clamping diameter [mm]	80
Diameter impact point [mm]	16	20
Temperature chamber?	no	Yes

(diameter 40 mm) and a larger hemispherical impact point (diameter 20 mm). Plate size was 100 × 100 mm.

The setup with the small clamping frame was equipped with a temperature chamber to test specimens at lower temperatures (after temperature equilibration). The tests were performed following ISO 6603-2. The contact force, impactor displacement and time were recorded at a sampling rate of 200 kHz.

For both machines, load cell force data and laser displacement sensor data, were logged on a data-logger and loaded into a home-made computer program to analyze the results. Low-velocity-impact resistance was determined as the energy absorbed at full penetration of the composite plate, calculated by the difference in kinetic energy of the striker before and after the impact of the composite plate. Tests were performed at full penetration, to find the proper energy for this, where necessary the incident energy was increased. Full penetration means that the striker went fully through the plate, and the remaining velocity after penetration could be measured from the displacement–time data. Penetration impact energies are always normalized to plate thickness to filter out the effect of volume of material present. To minimize the effect of difference in plate bending stiffness, all plates were produced at 2 mm thickness. For each material typically four specimens were tested.

To verify the accuracy of the kinetic energy method, as a standard also the penetration energy is calculated from the force displacement data, by taking the energy up to the point that the impact force falls back to 50% of the maximum load. When the value was calculated this way, it was never more than 15% different compared to the kinetic energy method; the difference can be attributed to friction energy.

Numerical results from both impact devices were never directly compared, because the response was determined by the geometries of the impact devices, and the setups were different. For instance, the setup with the temperature control used smaller plates, so the elastic bending response would be less and the impact penetration event more localized near the impactor.

2.4. Microscopy

A Philips CL30 series scanning electron microscope (SEM) was employed to image fracture surface topography after tensile testing of the epoxy and thermoplastic (0,90)_s silk weave composites. The surface was sputter coated with gold before imaging to obtain better contrast.

3. Results

3.1. Influence of Matrix and Fiber–Matrix Adhesion

Table 5 gives the results of the low-velocity-impact test in the impact setup 1 on (0,90)_s silk twill weave (2/2) composites with different polymer matrices, as well as the impact results for three selected unreinforced matrices. The absorbed impact energy per millimeter thickness ranges from 2 J mm⁻¹ for the epoxy composite up to 44 J mm⁻¹ for the PTMAT composite.

Figure 1 evaluates the absorbed impact energies at full penetration against the elongation to failure of the polymer matrix.

Table 5. Results of impact tests to full penetration on (0,90)_s silk twill weave (2/2) composites with different matrices and on pure matrix (polymer) samples. Absorbed energy per millimeter plate thickness at full penetration, maximum force, and maximum deflection is included. Tests are performed on impact setup 1.

Polymer Matrix	Absorbed energy [J mm ⁻¹]	Max Force [N]	Max deflection [mm]
Epoxy	2 ± 0.5	/	/
PBS	32 ± 2.5	3100 ± 290	17 ± 1
PBSa	38 ± 3	3400 ± 210	19 ± 2
PCL	38.5 ± 0.5	3600 ± 330	17 ± 1
PTMAT	44 ± 2	3300 ± 280	21 ± 1
PLA	24.5 ± 2	2900 ± 180	12 ± 2
CoPP	25.5 ± 0.5	2600 ± 180	15.5 ± 0.5
PP	30.3 ± 2.1	/	19 ± 1
PP-g-MA	15.5 ± 0.5	2150 ± 50	11.9 ± 0.6
HDPE-MA	23 ± 2	2400 ± 180	15 ± 1
Pure matrices:			
PP	4.1 ± 0.9	1750 ± 180	12.4 ± 1.3
PP-g-MA	10.8 ± 0.1	1630 ± 20	18.6 ± 0.6
HDPE-MA	9.0 ± 0.2	1300 ± 50	18.6 ± 0.5

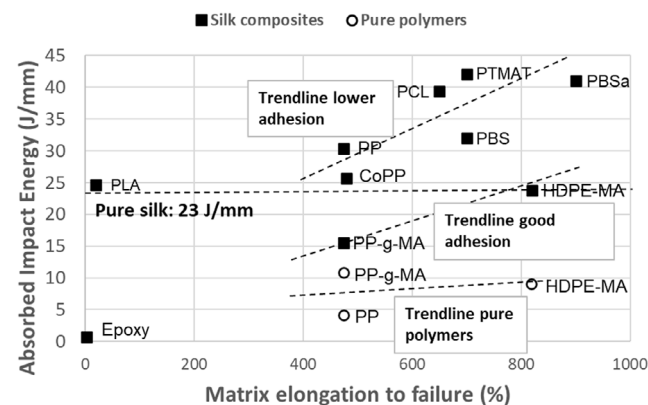


Figure 1. Absorbed impact energy at full penetration of (0,90)_s silk twill weave (2/2) composites as function of the ultimate elongation to failure of the matrix material for different polymer matrices. Measured on setup 1. As a reference, the measured value for the dry silk weave is included, as well as measured values for a few pure polymer plates.

A general trend is seen for the composites with the absorbed impact energy at full penetration increasing with increasing strain to failure of the polymer matrix. In case of the brittle (and relatively well adhering) epoxy, the toughness of the silk fiber is lost and the composite is not impact resistant. Impregnating the silk fibers in a tougher thermoplastic matrix increases the absorbed energy at full penetration dramatically. The higher absorbed energy is accompanied by a higher deflection of the composites before break as indicated in Table 5. Figure 2 shows the force–displacement curves recorded during the low-velocity-impact test for some of the different thermoplastic matrices. It can be seen that choosing a tougher thermoplastic

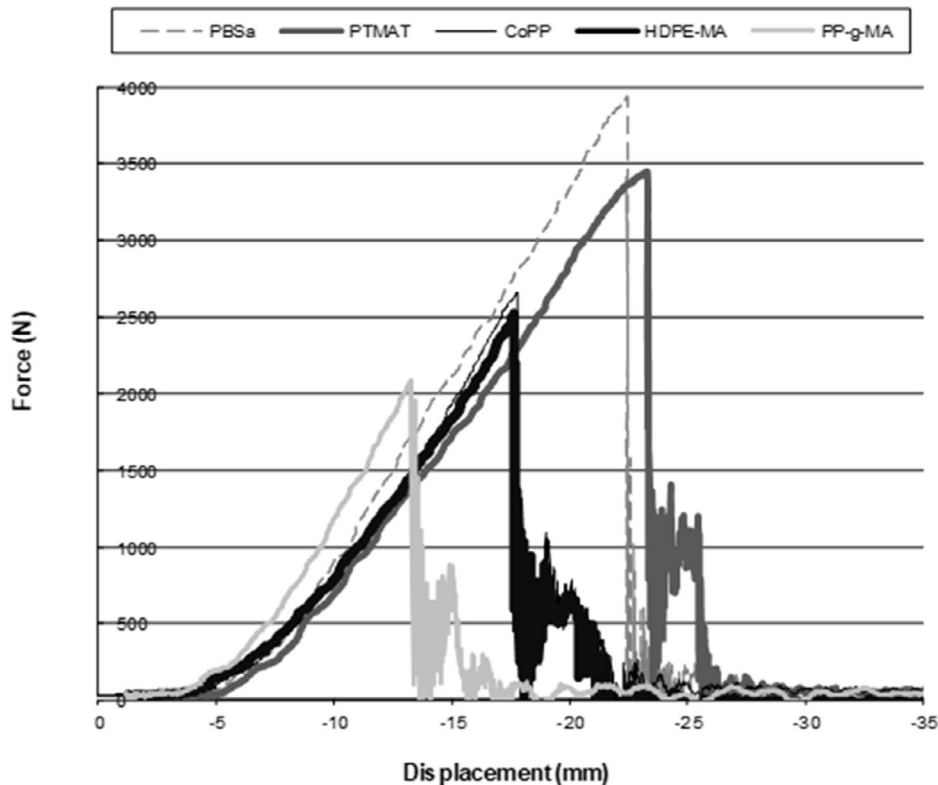


Figure 2. Force-displacement curves as measured during low-velocity-impact testing to full penetration. Results are illustrated for $(0,90)_s$ silk twill weave (2/2) composites with different thermoplastic matrix materials. Impact measurements were done on setup 1.

matrix like PBSa or PTMAT leads to higher deformations before penetration and higher maximum forces, and thus to higher energy absorption. This also accounts for the better adhering MA-modified polyolefins, but here the effect of the increased adhesion is to lower force and displacement, as is discussed later.

There is a combination of explanations for these effects. Due to the fact that the silk fibers are surrounded by a matrix with a high strain to failure, the fibers will eventually fail first and it is possible to exploit their high toughness to the full. That the effect keeps increasing even toward matrices with very high strain to failures may be attributed to the fact that during impact, material will also be loaded in direction transverse to the fibers, with the matrix and interface experiencing the same stress as the fibers in transverse direction; if the matrix has a high strain to failure, failure can be postponed, certainly in a woven or cross-ply structure, where there are also fibers present in transverse orientation (in other plies).

On top of the better utilization of the toughness of the fibers, there will be an additional contribution of the matrix itself. The extra effects of debonding, fiber pullout, and delamination as a function of interface strength will be discussed later. Impact tests were also performed on three different unreinforced matrices (see Table 5 and Figure 1). The penetration impact energy remained below 11 J mm^{-1} . With a penetration impact resistance for the dry silk fabric determined at 23 J mm^{-1} (see later), a volumetric rule of mixtures would predict a composite penetration resistance of maximum 17 J mm^{-1} . As can be seen, this is about what is measured for the PP-g-MA matrix, but for all other

polymer matrices, the impact energy is considerably to much higher, pointing at additional energy absorbing mechanisms.

It is suggested that there is a considerable influence of the adhesion between the silk fiber and the thermoplastic matrix as indicated in Figure 1. Adhesion strength between the silk fiber and the polymer matrix was qualitatively evaluated using the SEM pictures shown in Figure 3. These SEM pictures were taken of broken tensile specimens of the $(0,90)_s$ silk twill weave (2/2) composites, tested in warp direction.^[2] For the epoxy and the PP-g-MA composites, the matrix still adheres to the silk fibers. For the Co-PP composites, the silk fibers are dry and there is no polymer matrix left on the fibers, indicating relatively low adhesion. The adhesion between the silk fibers and PBS is somewhere in between.

The maleic anhydride-modified thermoplastic matrices, like PP-g-MA and HDPE-MA, show a good adhesion with the silk fibers, as could be expected due to the chemical adhesion between the ring-opened MA groups (carboxylic acid groups) and OH groups on the silk fiber. This leads to less debonding and fiber pullout and also, plausibly, to less delamination. All these effects will lead to more localized damage (see also the lower deflection during impact) with less volume available for plastic deformation. At similar adhesion strength, the above discussed effect of the strain to failure of the polymer matrix is still clearly present when comparing PP-g-MA and HDPE-MA.

For the epoxy composites, the low impact resistance has a double reason. One is the good adhesion of the silk fiber with the epoxy matrix; the second reason is the low elongation to failure of the epoxy matrix. In this way, the fiber does not detach

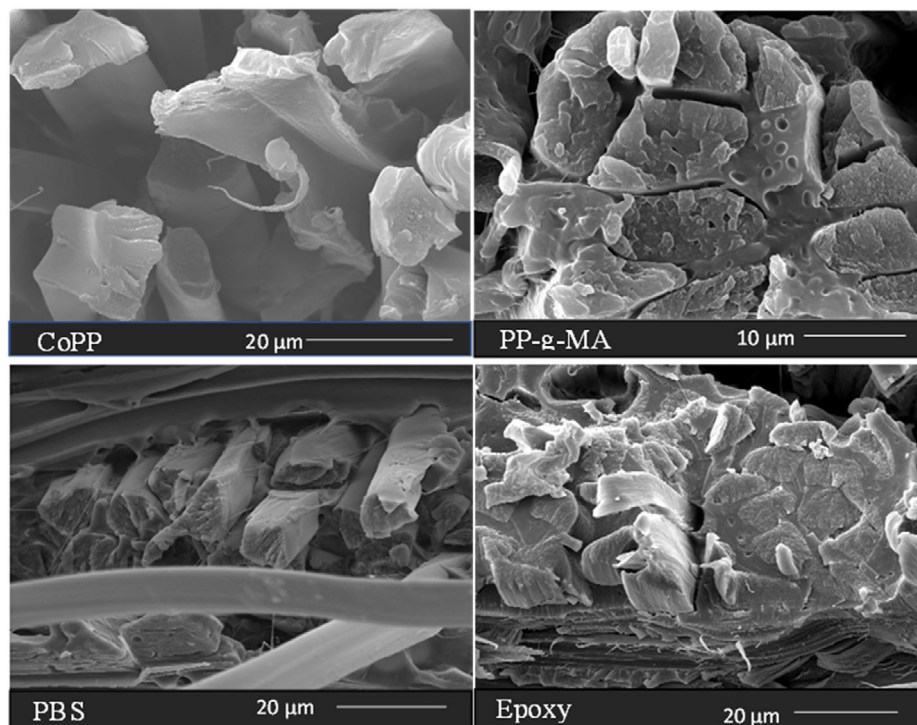


Figure 3. Scanning electron microscopy (SEM) of the fracture surfaces of (0,90)_s silk twill (2/2) weave composite tensile test specimens tested in the warp direction, to qualitatively reveal the degree of fiber–matrix adhesion. Fracture surfaces are shown for different polymer matrices as indicated on the picture.

from the epoxy matrix and fractures prematurely, initiated by the cracking of the brittle epoxy.

For the PLA composites, the absorbed impact energy at full penetration is high (25 J mm^{-1}) although the PLA matrix fails already at 4% strain. In this case, the reason is the bad impregnation of the hydrophobic PLA polymer matrix into the silk fibers. In this way, the silk weave and the PLA matrix behave separately. The matrix fails in a brittle way but debonds completely and immediately from the silk weave. In this way, the matrix cracks are blunted and the silk fibers can deform to their full capacity. The absorbed energy at full penetration is in this case similar to the value measured for dry silk weaves. This latter value was measured by taking the same amount of dry silk fabrics as in the composite (effectively creating a system with the same thickness and thus in a way a fiber volume fraction of about 50% in air). Again, the energy was measured to completely perforate the stack of fabrics. Of course, a layer of fabrics will interact differently with each other (through friction) than a composite where the stress is transferred between layers via the polymer matrix, but this way an indication is obtained how much energy it takes to just perforate a stack of dry fabrics.

3.2. Influence of Temperature

Figure 4 gives the absorbed energies for PBS, PP-g-MA, and HDPE-MA (0,90)_s silk twill weave (2/2) composites as measured in low-velocity-impact tests performed on setup 2. This setup is

equipped with a temperature chamber to cool down the composites to lower temperatures.

Figure 4 also shows the temperature at which the silk fiber composites were fully penetrated. Due to the high impact resistance and the limited capacity of the impact apparatus, the composites could not be penetrated on setup 2 at room temperature except for the PP-g-MA composites. This means that for the not penetrated samples the values in **Figure 4** are underestimations of the true penetration resistance. At lower temperature, also the PBS and HDPE-MA composites were fully penetrated. **Figure 4** illustrates that the low-velocity-impact resistance decreases with decreasing temperature. For PP-g-MA composites, force displacement curves at different temperatures are shown in **Figure 5**. Decreasing temperatures result in lower maximum force and lower maximum deformation.

These effects can be explained, because the polymer matrix becomes more brittle with lower temperature, particularly below the glass-transition temperature. For PP-g-MA, the T_g is around -5°C as given in Table 3. Below the glass-transition temperature, the thermoplastic polymer also has a higher stiffness. Both effects are clearly visible in the force–displacement curves in **Figure 5**, although the stiffening effect is relatively modest. At room temperature, the maximum deformation is still high at 13.6 mm. Below 0°C , the maximum deformation drops to only 5 mm at -25°C . Although the stiffening effect is modest, it does lead to some localization of damage and less plastic deformation. Together with embrittlement of the matrix, this results in earlier fracture and lower absorbed energy at full penetration. It is clear

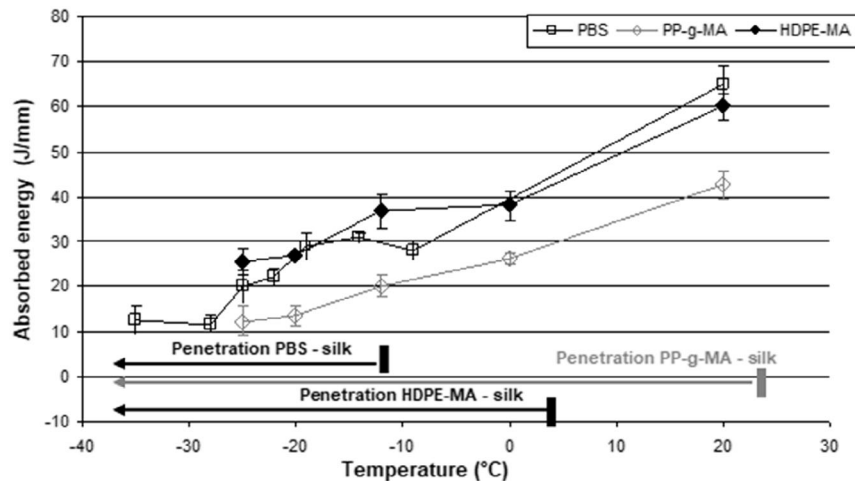


Figure 4. Absorbed energy of polybutylene succinate (PBS), maleic anhydride modified polypropylene (PP-g-MA) and maleic anhydride modified high-density polyethylene (HDPE-MA) (0,90)_s silk twill weave (2/2) composites impacted at different temperatures on setup 2. Only at lower temperatures, all silk fiber composites were penetrated depending on the matrix. The point where penetration started is indicated in the figure.

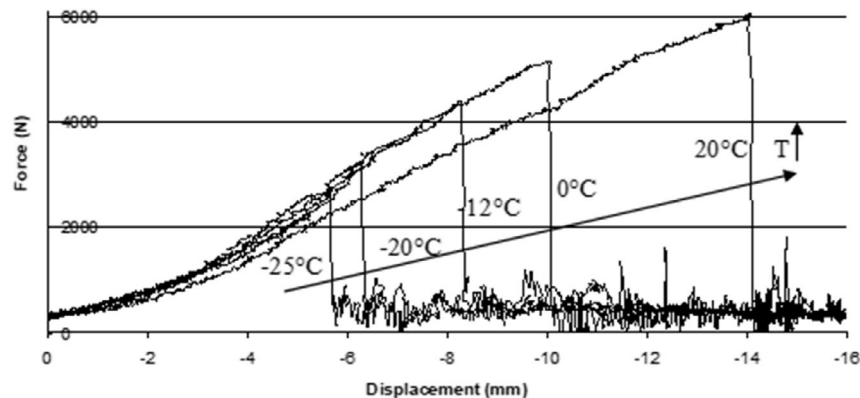


Figure 5. Force–displacement curves recorded during low-velocity-impact testing on PP-g-MA (0,90)_s silk twill weave (2/2) composites at different temperatures. Measurements were performed on impact setup 2.

that the glass-transition temperature of the polymer matrix is an important factor determining the brittleness of the polymer matrix. The glass-transition temperature of PBS is $-34\text{ }^{\circ}\text{C}$ and HDPE-MA has only a limited glass-transition due to the very high crystallinity. **Figure 6** compares the force-displacement curves of the (0,90)_s silk twill weave (2/2) composites with the three thermoplastic matrices at $-25\text{ }^{\circ}\text{C}$. Again, the relative brittleness of the PP-g-MA with the high glass-transition temperature at $-5\text{ }^{\circ}\text{C}$ is clearly visible.

3.3. Influence of Silk Fiber Architecture

In **Figure 7**, the impact penetration energy results are shown for various fiber architectures, all embedded in the high strain to failure PBSa matrix at around 50% fiber volume fraction.

The first remarkable effect is when instead of a balanced weave (twill weave [2/2]), an unbalanced weave is used (twill weave [5/3]). The impact resistance almost reduces by half. **Figure 8** shows what happens. The twill weave (2/2) composites

(**Figure 8a**) can undergo extensive deformation, before cracks develop in both the warp and weft directions of the fabric. In case of the unbalanced twill weave (5/3) composites (**Figure 8c**), cracks only develop in the weakest material direction with associated loss in energy absorption.

When the twill weave (5/3) fabrics are stacked in a balanced way, by alternately putting the weft or warp direction in the main direction of the plate, the composite strength becomes equal again in the main directions of the plate and the penetration impact resistance rises dramatically again (from 22 to 34 J mm^{-1}). The reason that the impact resistance of the twill weave (2/2) composite is not reached is probably because of the high twist of the weft yarns, lowering the strength.

Finally, **Figure 7** shows the performance of a quasi-isotropic layup of the twill weave (2/2) fabrics. The impact resistance is much lower than in case of the (0,90)_s twill weave (2/2) composite. **Figure 8b** shows that the fracture is more localized. It was shown in ref. [2], that in a quasi-isotropic layup, the extensive shearing of a woven composite when tested in the 45° direction is strongly reduced (17% versus about 40% failure strain). It is

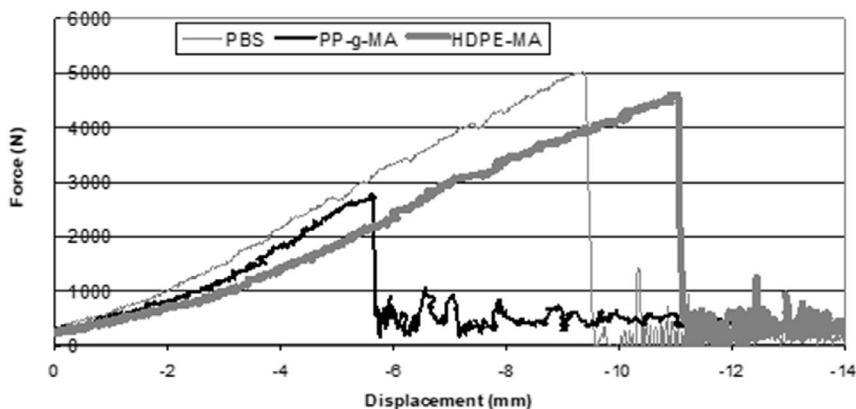


Figure 6. Force–displacement curves recorded during low-velocity-impact testing on PP-g-MA, HDPE-MA, and PBS (0,90)_s silk twill weave (2/2) composites at -25°C . Measurements were performed on impact setup 2.

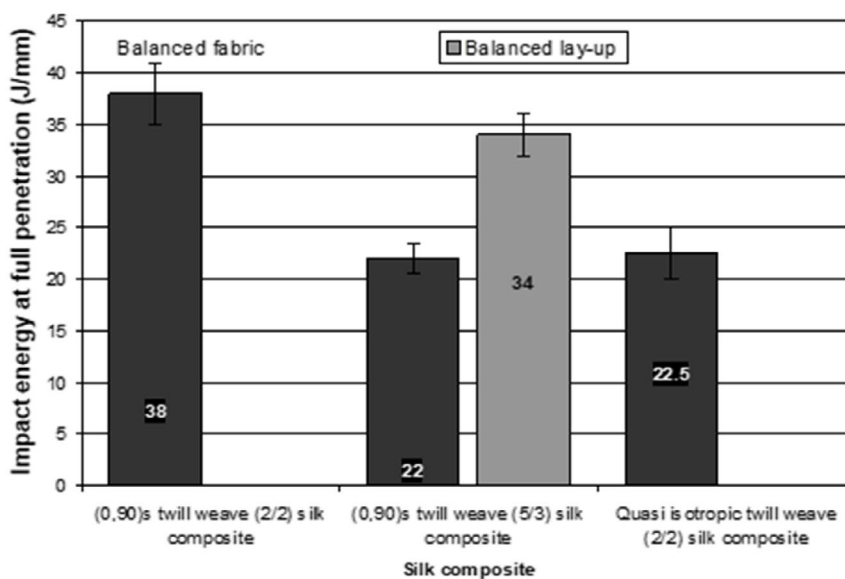


Figure 7. Absorbed impact energy to full penetration (J mm^{-1}) for different silk weave composites. Matrix material is always polybutyl succinate/adipate (PBSa). Measurements performed on impact setup 1. The grey bar indicates a balanced lay-up where the weft and warp directions are alternately aligned with the 0° direction. So in this case, the (0,90)_s silk weave (5/3) composite will have the same strength in both fiber directions.

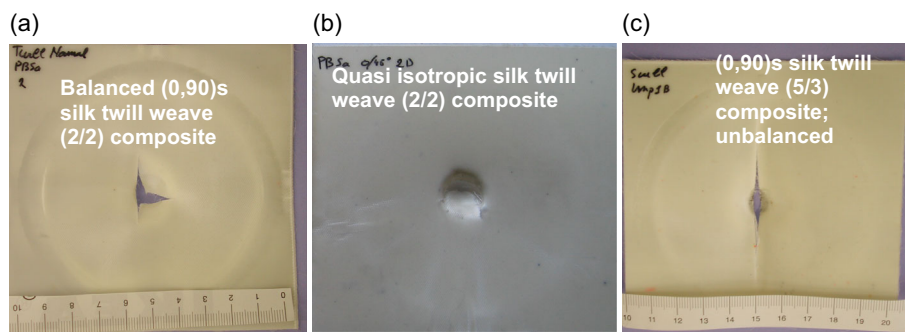


Figure 8. a) Different fracture modes for a (0,90)_s silk twill weave (2/2) composite, b) a quasi-isotropic silk twill weave (2/2) composite, and c) a (0,90)_s silk twill weave (5/3) composite (unbalanced). Matrix material is always PBSa.

hypothesized that the reduction in deformation, combined with reduced fiber failure due to the reduced fracture area is responsible for the lower impact resistance.

4. Conclusions

This research reveals the impact properties of silk weave composites when using different polymer matrices with a range of strains to failure and different levels of adhesion with the silk fiber. Furthermore, two different silk weaves, an unbalanced and a balanced variant, and two different layups, (0,90)_s and quasi-isotropic, were analyzed. The choice of the polymer matrix, the weave architecture, and the layup has a clear influence on the final low-velocity-impact properties of the silk weave composites. Following conclusions can be drawn for optimal low-velocity-impact performance of silk weave composites with different polymer matrix materials. 1) Low-velocity-impact properties are improved when the silk weaves are impregnated in a polymer matrix with a high elongation to failure. A high elongation to failure leads to an exceptionally high impact resistance. When impregnating the silk weaves in a brittle (and well adhering) thermoset material, the low-velocity-impact resistance drops dramatically, probably due to strong loss in plastic deformation of both fiber and matrix. 2) The adhesion strength between the silk fiber and the polymer matrix plays an important role in the low-velocity-impact behavior of the silk weave composites. A lower adhesion strength stimulates debonding, fiber pull out, and delamination and makes the silk weave composites more penetration impact resistant. An important mechanism is the spread of energy over a larger volume of the material. 3) The low-velocity-impact resistance lowers dramatically when the temperature drops toward and below the glass-transition temperature of the thermoplastic polymer matrix. The conclusion is the same as the first. A brittle polymer matrix reduces the impact resistance of silk weave composites. 4) The architecture of the silk weave plays an important role. The impact resistance of the (0,90)_s silk weave composites with an unbalanced silk weave as reinforcement is lower as only the weak direction of the material fails. A composite with a balanced weave deforms more uniformly and can absorb a lot of energy (when impregnated with a thermoplastic matrix of high strain to failure). 5) A quasi-isotropic layup of silk weave composites has a lower impact resistance as the deformation behavior of the four interacting plies (0, 90, +45, -45) is restricted and the development of damage is localized. For example, extensive shearing like in case of the (0,90)_s-only configuration is hindered.

This research may instigate research toward applications where the high low-velocity-impact resistance of the thermoplastic silk weave composites is of benefit. The intrinsic toughness of the silk fibers can clearly be exploited as reinforcement in thermoplastic matrices.^[24]

Conflict of Interest

The authors declare no conflict of interest.

Data Availability Statement

The data that support the findings of this study are available from the corresponding author upon reasonable request.

Keywords

fiber/matrix adhesion, impact, silk fibers, thermoplastic FRP composites, toughness

Received: January 18, 2023

Revised: July 19, 2023

Published online:

- [1] J. Pérez-Rigueiro, C. Viney, J. Llorca, M. Elices, *J. Appl. Polym. Sci.* **2000**, *75*, 1270.
- [2] A. W. Van Vuure, J. Vanderbeke, Y. Mosleh, I. Verpoest, N. El-Asmar, *Composites, Part A* **2021**, *147*, 106442.
- [3] D. U. Shah, D. Porter, F. Vollrath, *Compos. Sci. Technol.* **2014**, *101*, 173.
- [4] C. Wu, K. Yang, Y. Gu, J. Xu, R. O. Ritchie, J. Guan, *Composites A* **2019**, *117*, 357.
- [5] K. Yang, R. O. Ritchie, Y. Gu, S. J. Wu, J. Guan, *Mater. Des.* **2016**, *108*, 470.
- [6] K. Yang, J. Guan, K. Numata, C. Wu, S. Wu, Z. Shao, R. O. Ritchie, *Nat. Commun.* **2019**, *10*, 3786.
- [7] Y. Mosleh, D. Clemens, L. Gorbatikh, I. Verpoest, A. W. Van Vuure, *J. Reinf. Plast. Compos.* **2015**, *34*, 624.
- [8] P. W. R. Beaumont, P. G. Riewald, C. Zweben, *Foreign Object Impact Damage to Composites*, American Society of Testing and Materials (ASTM), Philadelphia **1987**, pp. 134–158.
- [9] W. Elber, in *NASA Conf.*, Vol. 2334, NASA Conference Publication, Hampton, VA **1984**, pp. 99–121.
- [10] M. O. W. Richardson, M. J. Wisheart, *Composites, Part A* **1996**, *27*, 1123.
- [11] K. Yang, Z. Wu, C. Zhou, S. Cai, Z. Wu, W. Tian, S. Wu, R. O. Ritchie, J. Guan, *Composites, Part A* **2022**, *154*, 106760.
- [12] W. J. Cantwell, J. Morton, *Composites* **1991**, *22*, 347.
- [13] D. Delfosse, A. Poursartip, *Composites, Part A* **1997**, *28*, 647.
- [14] D. Delfosse, A. Poursartip, B. R. Coxon, E. F. Dost, *Non-Penetrating Impact Behaviour of CFRP at Low and Intermediate Velocities. Composite Materials: Fatigue and Fracture*, ASTM STP 1230, Martin RH, ASTM, Philadelphia, USA **1995**.
- [15] B. Schrauwen, T. Peijs, *Appl. Compos. Mater.* **2002**, *9*, 331.
- [16] D. D. R. Cartié, P. E. Irving, *Composites, Part A* **2002**, *33*, 483.
- [17] A. R. Boccaccini, J. Ovenstone, P. A. Trusty, *Appl. Compos. Mater.* **1997**, *4*, 145.
- [18] T. W. Shyr, Y. H. Pan, *Compos. Struct.* **2003**, *62*, 193.
- [19] R. Park, J. Jang, *Polym. Test.* **2003**, *22*, 939.
- [20] J. K. Wells, P. W. R. Beaumont, *J. Mater. Sci.* **1985**, *20*, 1275.
- [21] M. V. Hosur, M. Adbullah, S. Jeelani, *Compos. Struct.* **2005**, *67*, 253.
- [22] A. W. Van Vuure, J. Vanderbeke, N. El-Asmar, I. Verpoest, in *Proc. ICCM-16*, Kyoto, July 2007
- [23] I. M. Ward, P. J. Hine, *Polymer* **2004**, *45*, 1413.
- [24] WO 2007-110758, I. Verpoest, A. W. van Vuure, N. El Asmar, J. Vanderbeke, *Silk Fibre Composites*, KU Leuven & Hermes Sellier, Geneva, Switzerland **2006**.